

# McMillan map and nonlinear Twiss parameters

T. Zolkin\*

*Fermilab, PO Box 500, Batavia, IL 60510-5011*

S. Nagaitsev†

*Fermilab, PO Box 500, Batavia, IL 60510-5011 and  
The University of Chicago, Chicago, IL 60637*

I. Morozov‡

*Budker Institute of Nuclear Physics, 11 Acad. Lavrentieva Pr., Novosibirsk, 630090 Russia*

(Dated: April 28, 2022)

In this article we consider two dynamical systems: the McMillan sextupole and octupole integrable mappings originally introduced by Edwin McMillan; the second one is also known as canonical McMillan map. Both of them are simplest symmetric McMillan maps with only one intrinsic parameter, the trace of the Jacobian at the fixed point. While these dynamical systems have numerous of applications and are used in many areas of math and physics, some of their dynamical properties have not been described yet. We fulfill the gap and provide complete description of all stable trajectories including parametrization of invariant curves, Poincaré rotation numbers and canonical action-angle variables.

In the second part we relate these maps with general chaotic map in McMillan-Turaev form. We show that McMillan sextupole and octupole mappings are first order approximations of dynamics around the fixed point, in a similar way as linear map and quadratic invariant (Courant-Snyder invariant in accelerator physics) is the zeroth order approximation (known as linearization). Finally we suggest the new formalism of nonlinear Twiss parameters which incorporate dependence of rotation number as a function of amplitude, in contrast to e.g. betatron phase advance used in accelerator physics which is independent of amplitude. Specifically in application to accelerator physics this new formalism is capable of predicting dynamical aperture around 1-st, 2-nd, 3-rd and 4-th order resonances for flat beams, which is critical for beam injection/extraction.

arXiv:2204.12691v1 [nlin.SI] 27 Apr 2022

---

\* zolkin@fnal.gov

† nsergei@fnal.gov

‡ i.a.morozov@inp.nsk.su

## CONTENTS

I. Introduction	3
II. McMillan sextupole and octupole mappings	4
A. Symmetries of invariants of motion	4
III. Stability of fixed points and 2-cycles.	
Bifurcation diagrams.	8
A. Sextupole map	8
B. Octupole map	10
IV. Dynamics of sextupole and octupole	
McMillan mappings	13
A. Sextupole map	13
1. Parametrization of individual curve	13
2. Action-angle variables and Pioncaré rotation number	14
B. Octupole map	15
1. Parametrization of individual curve	15
2. Action-angle variables and Pioncaré rotation number	15
V. Applications of McMillan map	17
A. McMillan map and perturbation theory	17
B. Nonlinear Twiss parameters	18
C. General accelerator lattice	20
VI. Summary	21
VII. Acknowledgments	21
A. Stability of fixed points and 2-cycles for	
McMillan sextupole and octupole mappings	22
B. Elliptic Lissajous figures	24
References	26

## I. INTRODUCTION

A generic dynamical system typically endures the presence of chaos. The motion is chaotic when there is an insufficient amount of integrals of motion, also known as invariants or conserved quantities. Such systems are difficult to analyze and known to be intractable problems, i.e. any practical solution might require too many computational resources to be useful due to its high sensitivity to initial conditions, rounding errors and external perturbations.

On the other hand, when the system possesses enough first integrals, it is known as *integrable* with quite simple and predictable dynamics. Historically, many completely integrable problems studied in physics played an important role in further understanding more realistic and complicated scenarios. For example: (i) a multi-dimensional harmonic oscillator works as a good approximation of small amplitude oscillations in a general nonlinear system, (ii) the Kepler problem gives a general understanding of, let's say, Earth's orbit while the entire solar system consists of many objects (many-body problem) and is highly chaotic, and (iii) planetary motion about two fixed centers has been used in the calculation of satellite trajectories in the gravitational field of the Earth [1–3], the acceleration of electrons in atomic collisions [4, 5], and, the calculation of the energy levels of the  $H_2^+$  [6].

In this article, we focus on another famous example known as McMillan integrable map [7]. Originally, it was proposed by Edwin McMillan as a simple accelerator lattice with one degree of freedom, consisting of linear optics (corresponding to simple linear transformation in phase space) and a special thin nonlinear lens (nonlinear vertical shear transformation). As later demonstrated by Suris [8], McMillan mapping is also one of the very few possible integrable symplectic transformations of the plane with analytic integral of motion; for the map in the form (1) invariant has to be either regular, exponential or trigonometric polynomial of degree two in coordinate and momentum.

Here we demonstrate that in fact, McMillan map is not only a model lattice, but can be related to the general planar symplectic map with chaotic dynamics as its first order approximation (Section V A); the zeroth order considers local stability of an equilibrium point, known as a linearization of the map. This fact helps to “integrate-out” additional nonlinear features of small amplitude oscillations, including dependence of frequency on action variable. As a consequence, we suggest the new concept of nonlinear Twiss parameters for accelerator physics which is the natural extension to the existing Courant-Snyder formalism (Section V B). The new “language” allows not only an understanding of amplitude-dependent shift of the betatron tune, but a prediction of dynamical aperture around isolated low order resonances, representing a nonlinear integrable model for slow resonant extraction of a flat beam (Section V C).

Finally, in first part of the article, we fill the gap in analytical results by providing a canonical transformation to action-angle variables (Section IV) and complimentary bifurcation diagrams for McMillan sextupole and octupole mappings (Section III); these are the simplest symmetric McMillan maps with only one intrinsic parameter and quadratic (sextupole) or cubic (octupole) nonlinearities. Octupole, and even more general asymmetric McMillan maps, have been studied in great detail, especially by Iatrou and Roberts [9] who provided parametrization of individual curves. However, explicit expressions for rotation number as a function of canonical action integral have been missing until now. This knowledge is critical in understanding underlying dynamics and design of integrable accelerator lattices with desirable properties. Additionally, these analytical results can be applied to more realistic integrable accelerator lattices based on McMillan map, e.g. they describe a particle with zero angular momentum in the integrable (in 4D phase space) accelerator ring with axially symmetric McMillan electron lens [10].

## II. MCMILLAN SEXTUPOLE AND OCTUPOLE MAPPINGS

In this section we define two dynamical systems: *McMillan sextupole* and *McMillan octupole* integrable mappings. Both of them are in *McMillan-Turaev form* (or MT form for short), defined as:

$$\begin{aligned} \mathcal{M}_{\text{MT}} : \quad q' &= p, \\ p' &= -q + f(p). \end{aligned} \tag{1}$$

The sextupole map has a force function

$$f_{\text{sex}}(p) = -p \frac{p+2\epsilon}{p+\Gamma} = -\frac{2\epsilon}{\Gamma} p - \frac{\Gamma-2\epsilon}{\Gamma^2} p^2 + \frac{\Gamma-2\epsilon}{\Gamma^3} p^3 + \mathcal{O}(p^4). \tag{2}$$

The first nonlinear term in the power series is quadratic, corresponding to the thin sextupole lens. When  $f(p) = ap + bp^2$ , the map is non-integrable and is known as the *area-preserving Hénon quadratic map*, [11]. In Section V we provide the relation between general map in MT form (including Hénon and Chirikov maps) and McMillan sextupole and octupole mappings as its approximation.

The octupole map is sometimes referred to as *canonical McMillan Map* (see [9]) with

$$f_{\text{oct}}(p) = -\frac{2\epsilon p}{p^2 + \Gamma} = -\frac{2\epsilon}{\Gamma} p + \frac{2\epsilon}{\Gamma^2} p^3 - \frac{2\epsilon}{\Gamma^3} p^5 + \mathcal{O}(p^7). \tag{3}$$

Now the first nonlinear term is cubic, corresponding to the thin octupole lens. We suggest these names in order to reflect the dynamical nature of systems. This integrable map approximates general mappings of the form (1) when  $f(p)$  is an odd function, or more generally when  $\partial_{pp}f(p) = 0$ .

### A. Symmetries of invariants of motion

The invariant of motion for the sextupole map in matrix form is

$$\begin{bmatrix} p^2 \\ p \\ 1 \end{bmatrix}^T \left( \begin{bmatrix} 0 & 1 & \Gamma \\ 1 & 2\epsilon & 0 \\ \Gamma & 0 & -\mathcal{K} \end{bmatrix} \cdot \begin{bmatrix} q^2 \\ q \\ 1 \end{bmatrix} \right) = p^2 q + p q^2 + \Gamma (p^2 + q^2) + 2\epsilon p q - \mathcal{K} \equiv 0,$$

or explicitly

$$\mathcal{K}_{\text{sex}}(p, q) = p^2 q + p q^2 + \Gamma (p^2 + q^2) + 2\epsilon p q.$$

The following propositions are straightforward to verify.

**Proposition A.1** *Simultaneous change of map parameters ( $\epsilon \neq 0$ )*

$$\Gamma \rightarrow \epsilon \Gamma, \quad \epsilon \rightarrow \epsilon \epsilon,$$

*along with the scaling transformations*

$$(p, q) \rightarrow \epsilon (p, q) \quad \text{and} \quad \mathcal{K} \rightarrow \epsilon^3 \mathcal{K}$$

*leaves the form of the map and biquadratic invariant.*

**Proposition A.2** *Simultaneous change of map parameters*

$$\Gamma \rightarrow \frac{\Gamma - 2\epsilon}{3}, \quad \epsilon \rightarrow -\frac{4\Gamma + \epsilon}{3},$$

*along with the translation transformations*

$$(p, q) \rightarrow (p, q) + \frac{2}{3} (\Gamma + \epsilon) \quad \text{and} \quad \mathcal{K} \rightarrow \mathcal{K} - \left[ \frac{2}{3} (\Gamma + \epsilon) \right]^3$$

*leaves the form of the map and biquadratic invariant.*



There are two consequences from the first proposition. First, there is only one intrinsic parameter — the ratio of  $\epsilon$  and  $\Gamma$ ; in a space of map parameters  $(\Gamma, \epsilon)$ , all dynamical systems on a ray  $\epsilon/\Gamma = \text{const}$  that starts at the origin, are similar up to the scaling transformation. In fact, this parameter is the trace of Jacobian evaluated at the fixed point at the origin,  $\zeta^{(1-1)} = (0, 0)$ ,

$$\text{Tr } J_{\text{sex}}(\zeta^{(1-1)}) = -\frac{2\epsilon}{\Gamma} = a.$$

Second, Proposition A.1 tells us that if we know the dynamics on a ray  $\epsilon/\Gamma = \text{const}$ , the dynamics for the systems on the opposite ray,  $\Gamma \rightarrow -\Gamma$  and  $\epsilon \rightarrow -\epsilon$ , is given by the rotation of the phase space by an angle of  $\pi$  and inversion of  $\mathcal{K}$ , (case  $\varepsilon = -1$ ).

The second proposition shows that there is a discrete symmetry with respect to the choice of origin; translation

$$(p, q) \rightarrow (p, q) - \zeta^{(1-2)}$$

shifts the origin to the second fixed point located on the main diagonal

$$\zeta^{(1-2)} = -\frac{2}{3}(1, 1)(\Gamma + \epsilon).$$

The transformation of parameters

$$\begin{bmatrix} \Gamma \\ \epsilon \end{bmatrix} \rightarrow \begin{bmatrix} \frac{1}{3} & -\frac{2}{3} \\ -\frac{4}{3} & -\frac{1}{3} \end{bmatrix} \begin{bmatrix} \Gamma \\ \epsilon \end{bmatrix},$$

is an inversion ( $\det = -1$ ) with two eigenvectors: the eigenvector along the line  $\epsilon = -\Gamma$  with unit eigenvalue

$$v_1 = (-1, 1)/\sqrt{2}, \quad \lambda_1 = 1,$$

and another eigenvector with minus unit eigenvalue and along the line  $\epsilon = 2\Gamma$

$$v_2 = (1, 2)/\sqrt{5}, \quad \lambda_2 = -1.$$

Both eigenvectors are related to symmetries between fixed points  $\zeta^{(1-1,2)}$ . For all dynamical systems along the line  $\epsilon = -\Gamma$ , fixed points  $\zeta^{(1-1,2)}$  undergo transcritical bifurcation and degenerate to a single point. When  $\epsilon = 2\Gamma$ , the phase space portrait of such dynamical systems has mirror symmetry with respect to line  $p = -q - \frac{1}{2}$ , and,  $\zeta^{(1-1,2)}$  are mirror images of each other. Without loss of generality, as a result of Propositions A.1–A.2, we will consider the dynamics only for the area of parameters (sector I in Fig. 1)

$$(\epsilon > -\Gamma) \cap (\epsilon < 2\Gamma) \quad \text{or} \quad a \in [-4; 2], \quad \Gamma \geq 0.$$

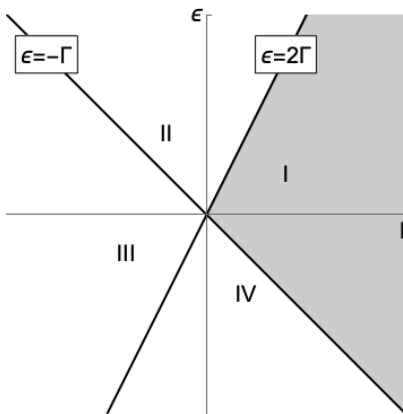


FIG. 1. Symmetry lines on the  $(\Gamma, \epsilon)$ -plane for McMillan sextupole map. Dynamics in sectors I and III (II and IV) are related through the Proposition A.1. Dynamics in sectors I and IV (II and III) are related through the Proposition A.2. Filled region shows the area of considered parameters.

The invariant of motion for the octupole map is

$$\begin{bmatrix} p^2 \\ p \\ 1 \end{bmatrix}^T \left( \begin{bmatrix} 1 & 0 & \Gamma \\ 0 & 2\epsilon & 0 \\ \Gamma & 0 & -\mathcal{K} \end{bmatrix} \cdot \begin{bmatrix} q^2 \\ q \\ 1 \end{bmatrix} \right) = p^2 q^2 + \Gamma(p^2 + q^2) + 2\epsilon p q - \mathcal{K} \equiv 0,$$

or

$$\mathcal{K}_{\text{oct}}(p, q) = p^2 q^2 + \Gamma(p^2 + q^2) + 2\epsilon p q,$$

with the following propositions

**Proposition A.3** *Simultaneous change of map parameters ( $\epsilon > 0$ )*

$$\Gamma \rightarrow \epsilon \Gamma, \quad \epsilon \rightarrow \epsilon \epsilon,$$

along with the scaling transformations

$$(p, q) \rightarrow \sqrt{\epsilon}(p, q) \quad \text{and} \quad \mathcal{K} \rightarrow \epsilon^2 \mathcal{K}$$

leaves the form of the map and biquadratic invariant.

**Proposition A.4** *Change of the map parameter*

$$\epsilon \rightarrow -\epsilon,$$

along with the reflection with respect to  $p = 0$  (or  $q = 0$ ),

$$\begin{aligned} q' &= q \\ p' &= -p \end{aligned} \quad \left( \begin{array}{l} \text{or} \\ \end{array} \right. \quad \begin{aligned} q' &= -q \\ p' &= p \end{aligned} \quad (4)$$

leaves the biquadratic invariant.

As a result of the first proposition, similar to the sextupole case, the dynamics on ray  $\epsilon/\Gamma = \text{const}$  with initial point at the origin is identical up to the scaling transformation. While the system still has one intrinsic parameter  $a = -2\epsilon/\Gamma$ , in contrast to the sextupole case, we have two different forms of invariants for  $\Gamma \leq 0$ , since  $\epsilon$  is strictly positive.

The second proposition is less powerful, since it only guarantees the conservation of the form of the invariant but not the map. In fact, it can be accompanied by another proposition:

**Proposition A.5** *Change of the map parameter*

$$\epsilon \rightarrow -\epsilon,$$

influences the dynamics of stable trajectory on a given energy level,  $\mathcal{K} = \text{const}$ , as follows:

- The invariant curves  $\mathcal{K}(q, p) \rightarrow \mathcal{K}(q, -p) = \mathcal{K}(-q, p)$ .
- Symmetric fixed points transform to 2-cycle, and vice versa 2-cycle transforms to a pair of symmetric fixed points.
- Dynamics around fixed point at the origin transforms according to

$$\begin{aligned} J &\rightarrow J, \\ \nu &\rightarrow \frac{1}{2} - \nu, \end{aligned}$$

where  $J$  is the action and  $\nu$  is the rotation number.

△

- Obvious by direct substitution.

- In the next section it is shown explicitly by obtaining all fixed points and 2-cycles, but here we will provide some geometrical considerations. Due to the form of the map, all fixed points belong to the intersection of main diagonal  $p = q$  and second symmetry line  $p = f_{\text{oct}}(q)/2$ . All 2-cycles belong to the intersection of the second symmetry line with its inverse, i.e.  $q = f_{\text{oct}}(p)/2$ , and since  $f_{\text{oct}}$  is an odd function of its argument, the only solutions allowed belong to anti-diagonal  $p = -q$ . After the transformation  $(p, q) \rightarrow (-p, q)$ , corresponding critical points of the invariant from the main diagonal mapped to the anti-diagonal and vice versa. Additionally, it automatically follows from the next part of the proposition.
- Since after transformation (4) the area under the closed curve is preserved, it follows  $J \rightarrow J$ . The action can be seen as  $J = 2J' + 2J''$ , where  $J'$  is an area over  $2\pi$  in II and IV, and,  $J''$  is in I and III quadrants of  $(p, q)$ -plane. Using Danilov theorem [12, 13],  $\nu = dJ'/dJ$  and that after the transformation (4)  $J' \leftrightarrow J''$  one has:

$$\nu \rightarrow \frac{dJ''}{dJ} = \frac{d\left(\frac{J}{2} - J'\right)}{dJ} = \frac{1}{2} - \nu.$$

▽

Another way to see that both mappings have only one natural parameter is to notice that both force functions have singularities:  $p = -\Gamma$  for the sextupole and  $p = \pm\sqrt{\Gamma}$  for the octupole maps. Performing the non-dimensionalization by measuring  $q$  and  $p$  in units of  $\Gamma$  or  $\sqrt{|\Gamma|}$  for the sextupole and octupole maps respectively, one obtains

$$\mathcal{K}_{\text{sex}}(q, p)/\Gamma^3 = \Sigma \Pi + \text{C.S.}$$

and

$$\mathcal{K}_{\text{oct}}(q, p)/|\Gamma|^2 = \Pi^2 \pm \text{C.S.}, \quad \text{for } \Gamma \gtrless 0,$$

where  $\Sigma = p + q$  and  $\Pi = pq$  are symmetric combinations of dynamic variables and

$$\text{C.S.} \equiv p^2 + \frac{2\epsilon}{\Gamma} pq + q^2 = p^2 - apq + q^2 = \Sigma^2 - (a+2)\Pi$$

is the *Courant-Snyder term*. Now nonlinear terms appear with unit coefficients and the only parameter left is the trace of Jacobian at the origin  $a$ .

### III. STABILITY OF FIXED POINTS AND 2-CYCLES. BIFURCATION DIAGRAMS.

*Fixed point* ( $n = 1$ ) and *n-cycle* of the map  $\mathcal{M}$ ,  $\zeta^{(n)} \equiv (q, p)$ , are defined by  $\mathcal{M}^n(q, p) = (q, p)$ . Stability of  $n$ -cycle is given by the trace of Jacobian,  $|\text{Tr } J[\mathcal{M}^n(\zeta^{(n)})]| < 2$ . Analysis of isolated  $n$ -cycles of the map plays a critical role in understanding its bifurcations. Iatrou and Roberts [9] proved that for an integrable map with a smooth integral, isolated critical points of the integral belong to (isolated) cycles of the map and the points of isolated cycles of the map are (isolated) critical points of the integral. Applying it to a general asymmetric McMillan map, one can verify that invariant of motion can have up to 5 isolated critical points. Without a loss of generality, we assume that one of them corresponds to a fixed point at the origin. Four other critical points have to be fixed points as well, or, two of them can form an isolated 2-cycle. In an exceptional case these fixed points and 2-cycles can appear on the same level of invariant and then form 3- or 4-cycles; then, the map degenerates to a linear and, in fact, all orbits (except fixed point at the origin) become periodic with corresponding periods 3 and 4. Below we will consider bifurcations of the sextupole and octupole McMillan mappings.

For the mapping in McMillan form, fixed points belong to the main diagonal  $p = q$  and are given by the intersection of two symmetry lines

$$p = q \quad \text{and} \quad p = f(q)/2.$$

2-cycles are given by the intersection of the second symmetry line with its inverse

$$p = f(q)/2 \quad \text{and} \quad q = f(p)/2.$$

If  $f(q)$  is an odd function, then fixed points have to appear in symmetric pairs with respect to the origin and 2-cycles belong to intersection of anti-diagonal  $p = -q$  with  $p = f(q)/2$ .

#### A. Sextupole map

The sextupole map has two fixed points. The first one is at the origin

$$\zeta^{(1-1)} = (0, 0),$$

and an additional fixed point on the main diagonal is

$$\zeta^{(1-2)} = -\frac{2}{3}(\Gamma + \epsilon)(1, 1) = \frac{a - a_0}{3}(1, 1)\Gamma.$$

Both fixed points are defined for any values of parameters on  $(\Gamma, \epsilon)$ -plane. In addition, there is a 2-cycle

$$\begin{aligned} \zeta^{(2)} &= (\Gamma - \epsilon)(1, 1) \pm \sqrt{(\Gamma - \epsilon)(5\Gamma - \epsilon)}(1, -1) \\ &= \frac{1}{2} \left[ (a - a_{1/2})(1, 1) \pm \sqrt{(a - a_{1/2})(a - a_{1/2}^*)}(1, -1) \right] \Gamma, \end{aligned}$$

defined only in a sector  $(\Gamma - \epsilon)(5\Gamma - \epsilon) > 0$ . Stability analysis shows that 2-cycle is always unstable when  $\zeta^{(2)}$  is real, and is stable when  $\zeta^{(2)} \in \mathbb{C}^2$ .

A sophisticated version of the bifurcation diagram including level sets of invariant is presented in Fig 2. The plot shows  $(\Gamma, \epsilon)$ -plane (for  $\Gamma > 0$ ) with additional scale for  $a = -2\epsilon/\Gamma$  (added on the dash-dotted circle). Each ray on the diagram corresponds to the constant value of  $a$  and contour plots of invariant  $\mathcal{K}(p, q)$  are included, illustrating possible dynamical scenarios and bifurcations.

Stability and bifurcations of fixed points (2-cycles) are summarized in Fig. 3. The fixed point at the origin is stable for  $a_{1/2} = -2 < a < a_0 = 2$  (lower index for particular values of  $a_\nu$  is the corresponding rotation number  $\nu = \arccos(a/2)/(2\pi)$ ). When  $a = a_0$  it experiences transcritical bifurcation and exchange stability with  $\zeta^{(1-2)}$ . When  $a = a_{1/2}$ ,  $\zeta^{(1-1)}$  undergoes sub-critical period doubling bifurcation, the second fixed point also goes through sub-critical period doubling at  $a = a_{1/2}^* = -10$ . Finally, for  $a = a_{1/3} = -1$  the second fixed point and 2-cycle approach the same energy level and the map degenerates to a linear with  $f(p) = -p$  and all orbits around the origin have period equal to 3.

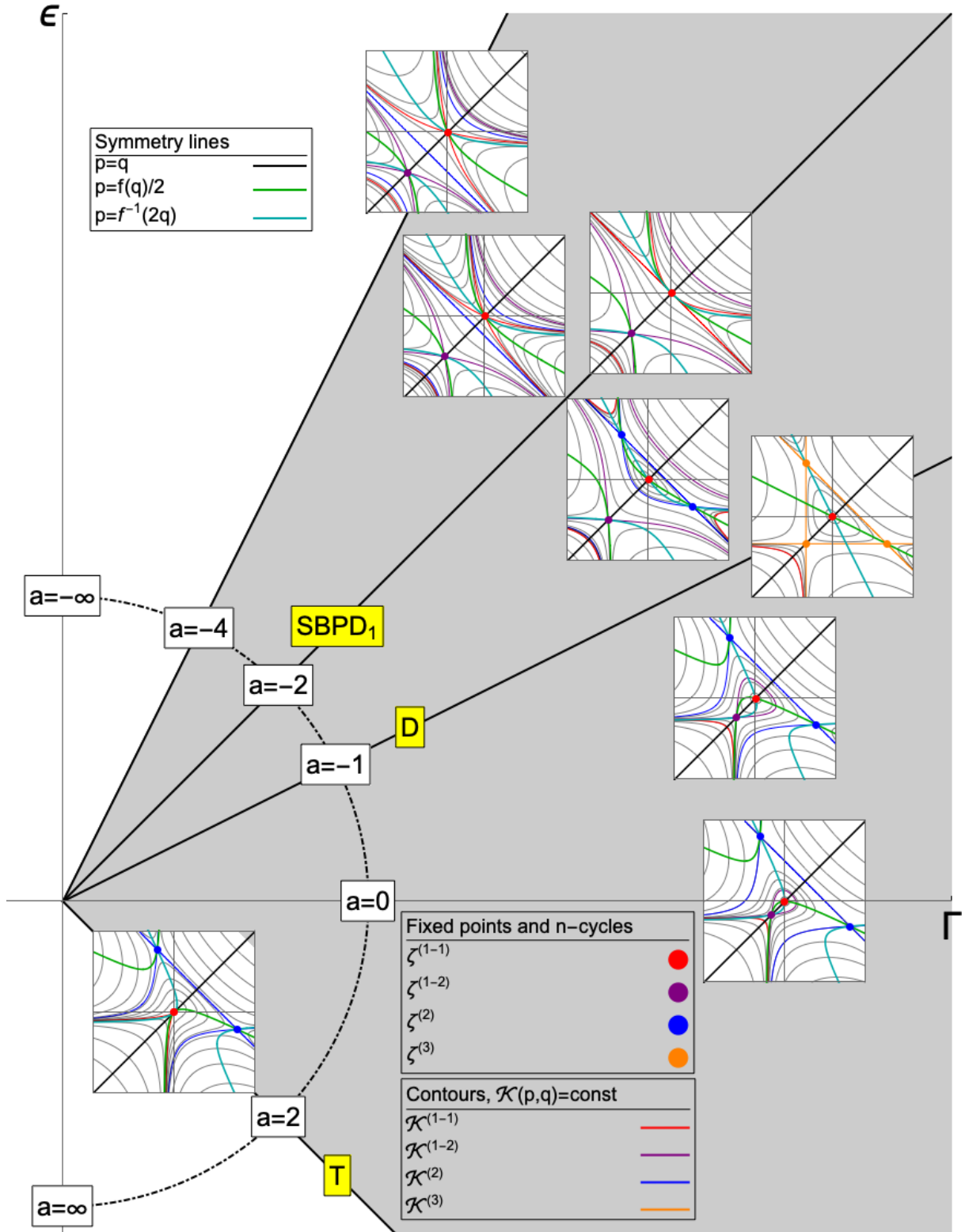


FIG. 2. Bifurcation diagram for the McMillan sextupole map.  $(\Gamma, \epsilon)$ -plane with rays of constant values of  $a = -2\epsilon/\Gamma$ . Sub-critical period doubling and transcritical bifurcations are marked with SBPD and T respectively. Label D corresponds to the system degeneracy. For each bifurcation (or in between) we provide characteristic contour plot of constant level sets of invariant. On each contour plot, fixed points, 2- and 3-cycles, as well as their corresponding level sets, are shown in colors according to the legend; other level sets are shown in black. First symmetry line  $p = q$ , second symmetry line  $p = f(q)/2$  and its inverse  $q = f(p)/2$  are shown in thick black, green and cyan respectively.

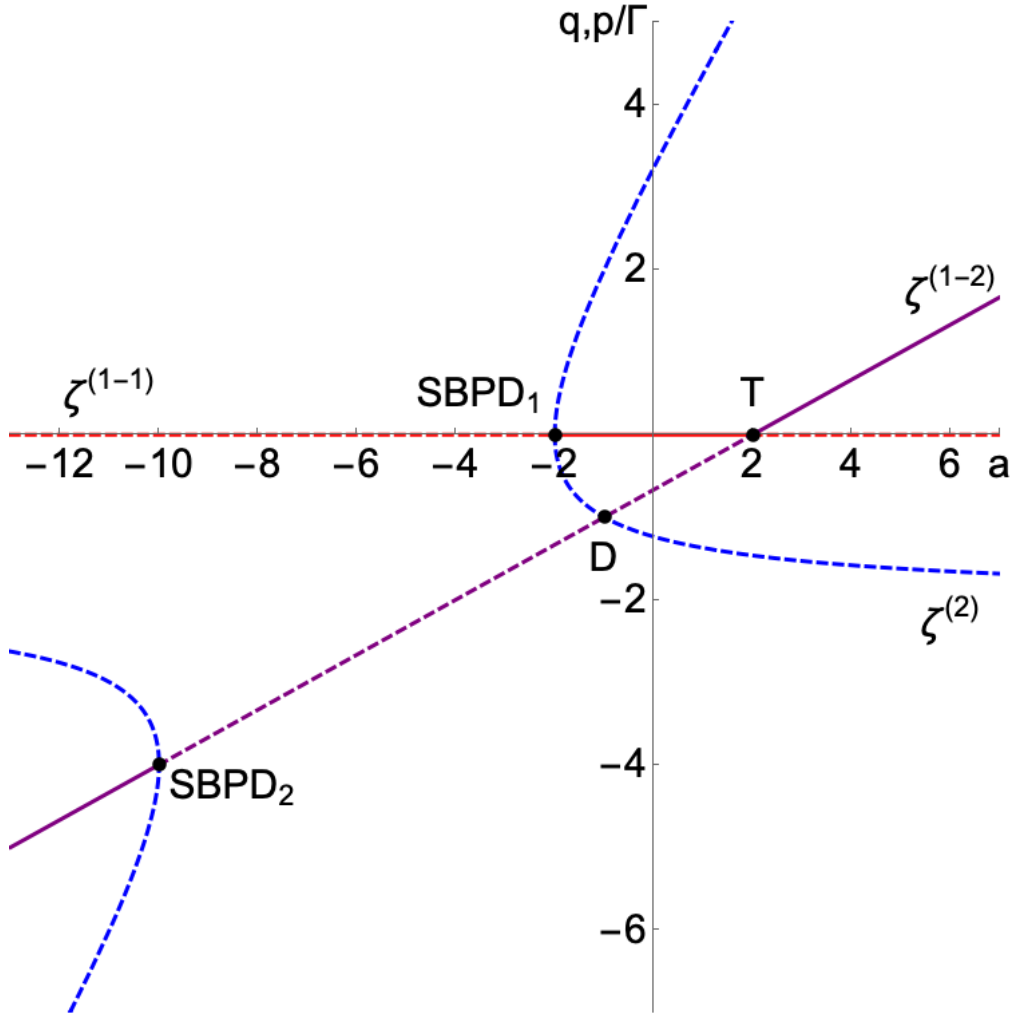


FIG. 3. Bifurcation diagram of fixed points and 2-cycles for the McMILLAN sextupole map. Plot shows normalized coordinates of 1,2-cycles as a function of parameter  $a = -2\epsilon/\Gamma$ . When fixed point or 2-cycle is stable (unstable) then it is shown as solid (dashed). Sub-critical period doubling and transcritical bifurcations are marked with SBPD and T respectively. Label D corresponds to the value of  $a = -1$  and represents system degeneracy.

### B. Octupole map

Similar to the sextupole case, the octupole map has a fixed point at the origin

$$\zeta^{(1-1)} = (0, 0),$$

which is again defined  $\forall(\Gamma, \epsilon) \in \mathbb{R}^2$  and stable for  $|\epsilon| < |\Gamma|$  (or  $a_{1/2} < a < a_0$ ). In contrast, it has two more fixed points appearing in a symmetric pair on the same energy level of the invariant

$$\zeta^{(1-2,3)} = \pm\sqrt{-(\Gamma + \epsilon)}(1, 1) = \pm\sqrt{\pm\frac{a - a_0}{2}}(1, 1)\sqrt{|\Gamma|}. \quad (5)$$

Note that the  $\pm$ -sign under the square root is for the cases  $\Gamma \geq 0$  (for both Eqs. (5,6)). Also note that in comparison to the sextupole map, the “natural” unit of distance is  $\sqrt{|\Gamma|}$  instead of  $\Gamma$ . Symmetric fixed points are defined only for  $\epsilon < -\Gamma$  (or  $a \geq a_0$  for  $\Gamma \geq 0$ ). A 2-cycle is defined for  $\epsilon > \Gamma$  (or  $a \leq a_{1/2}$  for  $\Gamma \geq 0$ ):

$$\zeta^{(2)} = \pm\sqrt{-(\Gamma - \epsilon)}(1, -1) = \pm\sqrt{\mp\frac{a - a_{1/2}}{2}}(1, -1)\sqrt{|\Gamma|}. \quad (6)$$

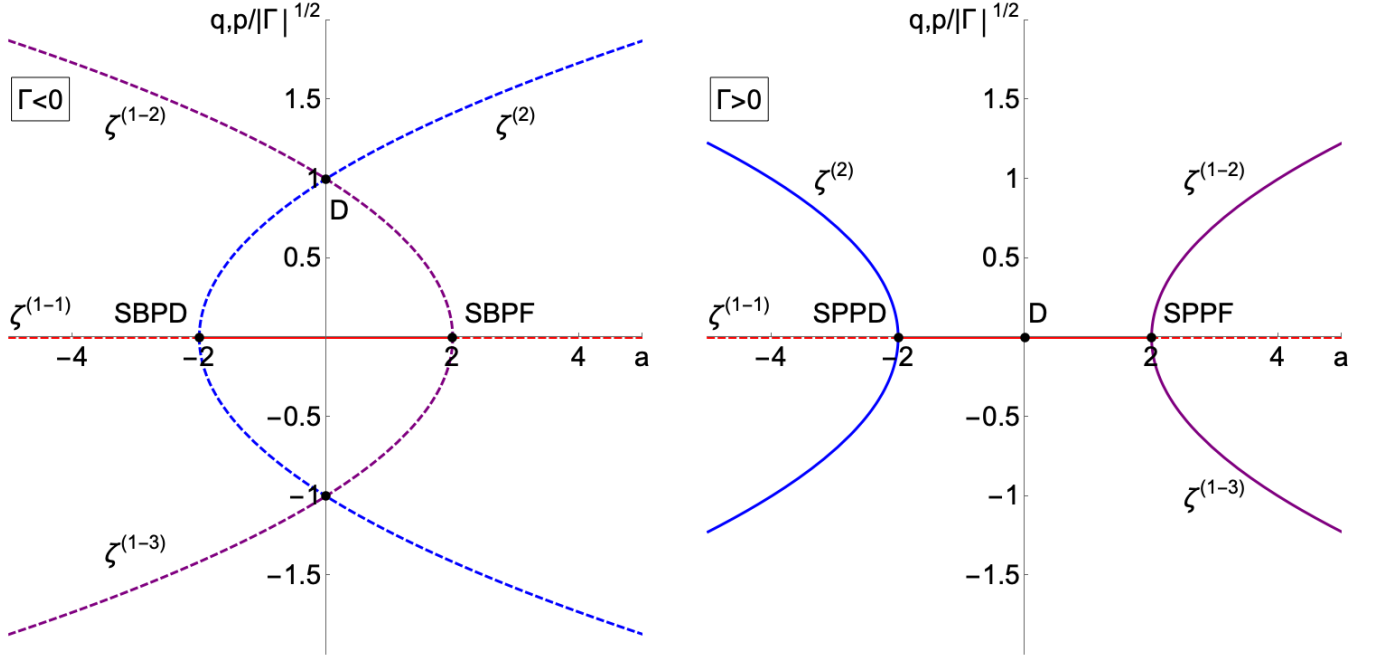


FIG. 4. Bifurcation diagram of invariant points and 2-cycles for the McMILLAN octupole map. Left and right plots show normalized coordinates of 1,2-cycles as a function of parameter  $a = -2\epsilon/\Gamma$  for  $\Gamma < 0$  and  $\Gamma > 0$  respectively. When fixed point or 2-cycle is stable (unstable) then it is shown as solid (dashed). Pitchfork and period doubling bifurcations are marked with PF and PD (SB for sub-critical and SP for super-critical). Label D corresponds to the value of  $a = 0$  and represents system degeneracy.

Stability and bifurcations plots for cases  $\Gamma \geq 0$  are presented in Fig. 4. When  $\Gamma < 0$  at  $a_{1/2,0}$  the fixed point undergoes sub-critical period doubling or pitchfork bifurcations respectively. Fixed points  $\zeta^{(1-2,3)}$  and 2-cycle  $\zeta^{(2)}$  are always unstable and the only region with stable trajectories is  $a_{1/2} < a < a_0$ . For  $\Gamma > 0$  at  $a_{1/2,0}$  the fixed point undergoes super-critical period doubling or pitchfork bifurcations. When  $\zeta^{(1-1)}$  is stable,  $a_{1/2} < a < a_0$ , there are no additional fixed points or 2-cycles and all trajectories are stable. When  $|a| > 2$ , all trajectories are globally stable again, but the point in the origin is locally unstable and becomes a center of lemniscate. If  $a > a_0$ , trajectories inside the figure-eight curve round the centers of “eyes,” while when  $a < a_{1/2}$  the orbit jumps from “eye” to “eye” since the centers become 2-cycles.

An additional bifurcation diagram with level sets of invariant is show below in Fig 5. Similar to the sextupole case, we use  $(\Gamma, \epsilon)$ -plane but now with two additional scales for  $a$  on each semi-plane  $\Gamma \geq 0$ . Each ray on a diagram corresponds to the constant value of  $a$  and contour plots of invariant  $\mathcal{K}(p, q)$  are included, illustrating possible dynamical scenarios and bifurcations.

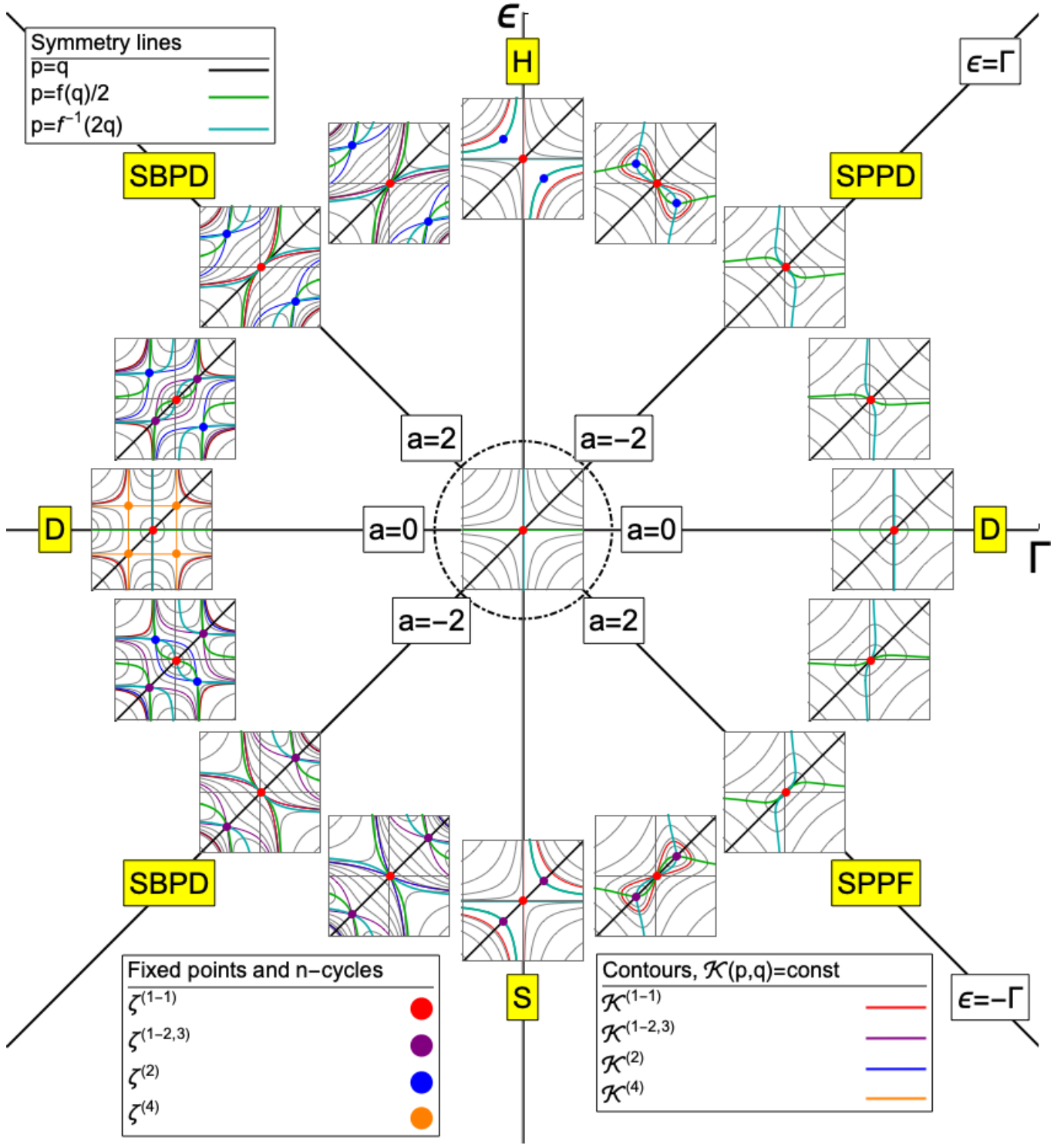


FIG. 5. Bifurcation diagram for the McMILLAN octupole map.  $(\Gamma, \epsilon)$ -plane with rays of constant values of  $a = -2\epsilon/\Gamma$  (one scale for each semi-plane  $\Gamma \geq 0$ ). Pitchfork and period doubling bifurcations are marked with PF and PD (SB for sub-critical and SP for super-critical). Label D corresponds to the system degeneracy. For each bifurcation (or in between) we provide characteristic contour plot of constant level sets of invariant. On each contour plot, fixed points, 2- and 4-cycles as well as their corresponding level sets are shown in colors according to the legend; other level sets are shown in black. First symmetry line  $p = q$ , second symmetry line  $p = f(q)/2$  and its inverse  $q = f(p)/2$  are shown in thick black, green and cyan respectively.



#### IV. DYNAMICS OF SEXTUPOLE AND OCTUPOLE MCMILLAN MAPPINGS

##### A. Sextupole map

###### 1. Parametrization of individual curve

Here we will illustrate the general method of obtaining a parametrization of an individual curve using the sextupole map as an example. We limit ourselves to cases with stable trajectories around the stationary point at the origin, considering only  $a_{1/2} < a < a_0$ . We start with a formal Hamiltonian system

$$\mathbb{H}[p, q; t] \equiv \mathcal{K}(p, q) = p^2 q + p q^2 + p^2 - a p q + q^2$$

which satisfies system of Hamilton's equations

$$\begin{aligned} \frac{dq}{dt} &= \frac{\partial \mathbb{H}}{\partial p} = q^2 - a q + 2p + 2p q, \\ -\frac{dp}{dt} &= \frac{\partial \mathbb{H}}{\partial q} = p^2 - a p + 2q + 2p q. \end{aligned}$$

Since Hamiltonian function does not change along the trajectory, we can solve for  $p$  from  $\mathbb{H} = \text{const}$ :

$$\begin{aligned} p &= \frac{q(a-q) \pm \sqrt{q^4 - 2(2+a)q^3 + (a^2-4)q^2 + 4\mathbb{H}q + 4\mathbb{H}}}{2(q+1)} \\ &= \frac{1}{2} \left[ f_{\text{sex}}(q) \pm \frac{\sqrt{\mathcal{P}(q)}}{q+1} \right], \end{aligned}$$

where

$$\mathcal{P}(q) = q^4 - 2(a - a_{1/2})q^3 + (a - a_0)(a - a_{1/2})q^2 + 4\mathbb{H}q + 4\mathbb{H}.$$

Substitution into the first Hamilton's equation gives

$$dt = \pm \frac{dq}{\sqrt{\mathcal{P}(q)}}. \quad (7)$$

When the fixed point at the origin is stable ( $a_{1/2} < a < a_0$ ), polynomial  $\mathcal{P}(q)$  has four distinct real roots such that

$$q_1 < q_2 \leq q \leq q_3 < q_4$$

and  $\mathbb{H} > 0$  for all closed invariant curves. Roots  $q_i$  satisfies

$$\sum_{i=1}^4 \frac{1}{q_i} = -1$$

and using Vieta's formulas for the quartic  $\mathcal{P}(q)$ , one can express map parameter and energy level using  $q_i$ :

$$a = -2 + \sum_{i=1}^4 q_i/2 \quad \text{and} \quad \mathbb{H} = \frac{1}{4} \prod_{i=1}^4 q_i.$$

Factorizing the polynomial,  $\mathcal{P}(q) = (q_4 - q)(q_3 - q)(q - q_2)(q - q_1)$ , we rewrite Eq. (7) as an integral

$$\int_0^t dt = \pm \int_{q_0}^q \frac{dq}{\sqrt{(q_4 - q)(q_3 - q)(q - q_2)(q - q_1)}}.$$

This is the standard integral which can be expressed in terms of any of three principal Jacobian elliptic functions

$$\begin{aligned} q(t) &= \frac{q_2 - q_1 \frac{q_3 - q_2}{q_3 - q_1} \text{sn}_1^2}{1 - \frac{q_3 - q_2}{q_3 - q_1} \text{sn}_1^2} = \frac{q_3 - q_4 \frac{q_3 - q_2}{q_4 - q_2} \text{sn}_2^2}{1 - \frac{q_3 - q_2}{q_4 - q_2} \text{sn}_2^2} \\ &= \frac{q_3 + q_1 \frac{q_3 - q_2}{q_2 - q_1} \text{cn}_1^2}{1 + \frac{q_3 - q_2}{q_2 - q_1} \text{cn}_1^2} = \frac{q_2 + q_4 \frac{q_3 - q_2}{q_4 - q_3} \text{cn}_2^2}{1 + \frac{q_3 - q_2}{q_4 - q_3} \text{cn}_2^2} \\ &= \frac{q_2 - q_1 \frac{q_4 - q_2}{q_4 - q_1} (1 - \text{dn}_1^2)}{1 - \frac{q_4 - q_2}{q_4 - q_1} (1 - \text{dn}_1^2)} = \frac{q_3 - q_4 \frac{q_3 - q_1}{q_4 - q_1} (1 - \text{dn}_2^2)}{1 - \frac{q_3 - q_1}{q_4 - q_1} (1 - \text{dn}_2^2)}, \end{aligned}$$

where  $\text{ef}_i$  is a shorthand notation for appropriate Jacobian function (elliptic sine  $\text{sn}$ , cosine  $\text{cn}$  or delta amplitude  $\text{dn}$ )

$$\text{ef}_i = \text{ef} \left[ \sqrt{(q_4 - q_2)(q_3 - q_1)} \frac{t - t_i^*}{2}, \kappa \right]$$

with modulus

$$\kappa = \sqrt{\frac{(q_3 - q_2)(q_4 - q_1)}{(q_4 - q_2)(q_3 - q_1)}},$$

and, two possible definitions of initial phases such that  $q(0) = q_0$ :

$$t_1^* = \frac{-2}{\sqrt{(q_4 - q_2)(q_3 - q_1)}} \text{F} \left[ \arcsin \sqrt{\frac{(q_3 - q_1)(q_0 - q_2)}{(q_3 - q_2)(q_0 - q_1)}}, \kappa \right],$$

$$t_2^* = \frac{2}{\sqrt{(q_4 - q_2)(q_3 - q_1)}} \text{F} \left[ \arcsin \sqrt{\frac{(q_4 - q_2)(q_3 - q_0)}{(q_3 - q_2)(q_4 - q_0)}}, \kappa \right].$$

## 2. Action-angle variables and Pioncaré rotation number

Now, we will relate continuous parametrization of invariant curves given by Hamiltonian with the mapping equations. First, we find the period of finite motion as

$$\text{T} \equiv \oint dt = 2 \int_{q_2}^{q_3} \frac{dq}{\sqrt{\mathcal{P}(q)}} = \frac{4 \text{K}[\kappa]}{\sqrt{(q_4 - q_2)(q_3 - q_1)}}.$$

Then we calculate the time of one-step

$$\begin{aligned} \text{T}' &\equiv \int_0^{\text{T}'} dt = \int_q^{q'} \frac{dq}{\sqrt{\mathcal{P}(q)}} = \int_{q_{2,3}}^{q'_{2,3}} \frac{dq}{\sqrt{\mathcal{P}(q)}} \\ &= \frac{2 \text{F}[\arcsin \sqrt{\frac{q_{3,4} - q_{1,2}}{q_3 - q_2} \frac{q_{2,3}(8 - q_1 + 5q_{2,3} - q_{3,2} - q_4)}{4q_{1,4} + q_{2,3}(4 + 3q_{1,4} + q_{2,3} - q_{3,2} - q_{4,1})}}, \kappa]}{\sqrt{(q_4 - q_2)(q_3 - q_1)}}, \end{aligned}$$

where we can choose either one of  $q_{2,3}$  as an initial coordinate, since the integral does not depend on initial phase on a given invariant curve, and, with the help of map equations we used

$$q'_{2,3} = p(q_{2,3}) = f(q_{2,3})/2 = -q_{2,3} \frac{q_{2,3} - a}{q_{2,3} + 1} = \frac{q_{2,3}(q_1 - q_{2,3} + q_{3,2} + q_4 - 4)}{4(q_{2,3} + 1)}.$$

Now we can rewrite the map in action-angle form

$$J' = J,$$

$$\theta' = \theta + 2\pi\nu.$$

The rotation number is defined as a ratio of the time of one-step over the period  $[\mathbf{N}]$

$$\nu = \text{T}'/\text{T} = \text{F} \left[ \arcsin \sqrt{\frac{q_3 - q_1}{q_3 - q_2} \frac{q_2(3q_2 + 2 - a)}{2q_1(q_2 + 1) + q_2(q_2 - a)}}, \kappa \right] / (2\text{K}[\kappa]).$$

The action is given by the integral

$$\begin{aligned} J &= \frac{1}{2\pi} \oint p dq = \frac{1}{2\pi} \int_{q_2}^{q_3} \frac{\sqrt{\mathcal{P}(q)}}{q+1} dq = \\ &= \frac{q_2 - q_1}{\pi} \sqrt{\frac{q_3 - q_1}{q_4 - q_2}} \left\{ \frac{a + 4 + q_4 - q_1}{4} \text{K}[\kappa] + \frac{a + 4}{4} \frac{q_4 - q_2}{q_2 - q_1} \text{E}[\kappa] - \right. \\ &\quad \left. - \frac{a + 1}{q_3 - q_1} \Pi \left[ \frac{q_4 - q_2}{q_4 - q_1} \kappa^2, \kappa \right] - \frac{(1 + q_3)(1 + q_4)}{q_3 - q_1} \Pi \left[ \frac{1 + q_1}{1 + q_2} \frac{q_4 - q_2}{q_4 - q_1} \kappa^2, \kappa \right] \right\}. \end{aligned}$$

The initial phase can be defined as  $\{\theta_0\} = \arctan(\{p_0\}/\{q_0\})$ . Right plot in Fig. 6 shows rotation number as a function of action for different values of  $a$ . In addition, Fig. 6 contains plots illustrating parametrization of invariant curve.

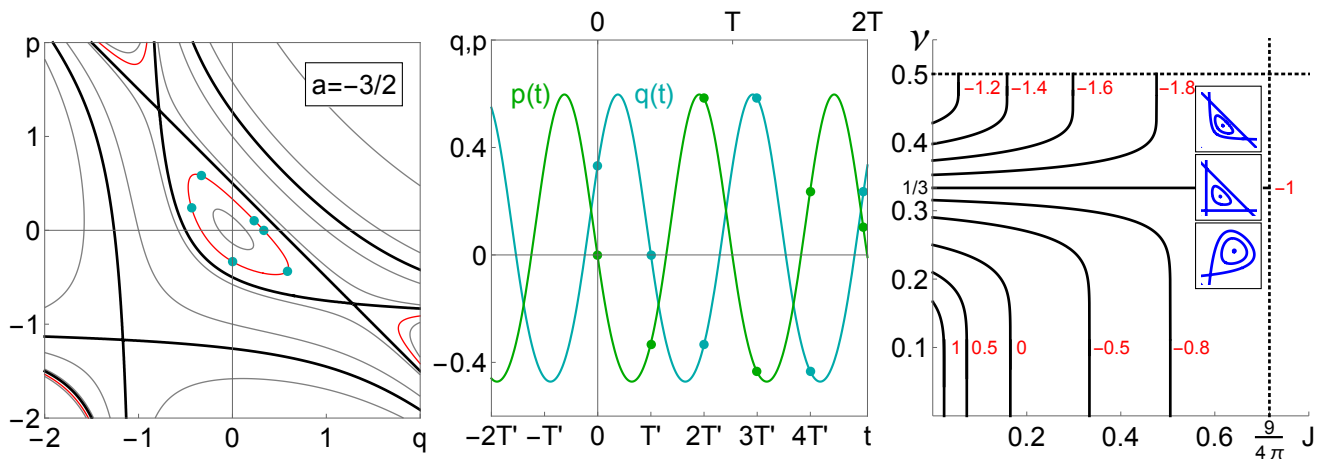


FIG. 6. Illustration to parametrization of invariant curve and action-angle variables for the McMillan sextupole map. Left plot shows invariant level sets  $\mathcal{K}_{\text{sex}}(q, p) = \text{const}$  for  $a = -3/2$  and  $\Gamma = 1$ . Thick black curves are level sets containing separatrices, isolated fixed point and 2-cycle. Red level set is used to illustrate parametrization. Cyan points on the closed red curve are first five iterations of initial condition  $(q_0, p_0) = (1/3, 0)$ . Middle plot shows continuous solution  $q, p(t)$  of Hamiltonian system with  $(q(0), p(0)) = (q_0, p_0)$  and sampled at the rate  $T'$  (time of one step); the time scale at the top is measured in periods of continuous system,  $T$ . Note that sampled points  $(q_n, p_n)$  match corresponding points on the red level set from the left plot. Plot on the right is the action-angle variables for different values of  $a$  (red labels).

## B. Octupole map

### 1. Parametrization of individual curve

For the octupole map, the parametrization of individual curves was done by Iatrou and Roberts in [9]. They also provided two different methods showing how an arbitrary constant level set of an asymmetric McMillan map can be transformed to canonical form,  $\mathcal{K}_{\text{oct}}(p, q)$ . Below we present their results using our notations and in the next section we find canonical action-angle variables.

Due to additional symmetries of the invariant, the functional dependence is much simpler compared to the sextupole case and all trajectories can be parametrized in a form

$$\begin{cases} q_n = \sqrt[4]{\mathcal{K}} h(\kappa) \text{ef}(u_0 + \eta_{\pm} n, \kappa), \\ p_n = q_{n+1} \end{cases}$$

where ef is an appropriate elliptic function with elliptic modulus  $\kappa$ ,  $h(\kappa)$  is amplitude,  $\eta_{\pm}$  is phase advance for  $a \geq 0$ , and  $u_0$  is initial phase defined by  $q_0$ .

For  $\Gamma < 0$ , appropriate elliptic function for stable trajectories is elliptic sine, sn. When  $\Gamma > 0$  one should use elliptic cosine, cn, or delta amplitude, dn, for trajectories rounding the origin or trajectories inside the lemniscate respectively. Expressions for all parameters are listed in Table I below (with  $\eta_- = 2\mathcal{K}[\kappa] - \eta_+$ ).

### 2. Action-angle variables and Poincaré rotation number

Note that in [9], the authors also defined action-angle variables which are not canonical: elliptic modulus  $\kappa$  is used as an action instead of an area under the curve and phase  $\eta$  is used instead of a rotation number.

The rotation number for trajectories rounding the origin or lemniscate (i.e. all sn and cn cases)

$$\nu = \frac{\eta}{4\mathcal{K}[\kappa]}$$

and for trajectories inside lemniscate orbiting one of the symmetric fixed points  $\zeta^{(1-2,3)}$  (dn case)

$$\nu = \frac{\eta}{2\mathcal{K}[\kappa]}.$$

	cn	dn	sn
$\mathcal{K} \in$	$[0; \infty) \geq 0$	$[-( \frac{a}{2}  - 1)^2; 0] \leq 0$	$[0; ( \frac{a}{2}  - 1)^2] \geq 0$
$B(a, \mathcal{K})$	$\frac{(a/2)^2 - 1 + \mathcal{K}}{\sqrt{ \mathcal{K} }}$ $= \frac{k}{k'} - \frac{k'}{k} \in \mathbb{R}$	$\frac{(a/2)^2 - 1 - \mathcal{K}}{\sqrt{ \mathcal{K} }}$ $= \frac{1}{k'} + k' \geq 2$	$-\frac{(a/2)^2 - 1 - \mathcal{K}}{\sqrt{ \mathcal{K} }}$ $= \frac{1}{k} + k \geq 2$
$k(B)$	$\frac{1}{\sqrt{2}} \sqrt{1 + \frac{B}{\sqrt{B^2 + 4}}}$	$\frac{\sqrt{B+2} - \sqrt{B-2}}{2(B^2 - 4)^{-1/4}}$	$\frac{B - \sqrt{B^2 - 4}}{2}$
$k'(B)$	$\frac{1}{\sqrt{2}} \sqrt{1 - \frac{B}{\sqrt{B^2 + 4}}}$	$\frac{B - \sqrt{B^2 - 4}}{2}$	$\frac{\sqrt{B+2} - \sqrt{B-2}}{2(B^2 - 4)^{-1/4}}$
$\eta_+$	$\operatorname{arccds} \frac{\sqrt{k k'}}{\sqrt[4]{ \mathcal{K} }}$	$\operatorname{arccs} \frac{\sqrt{k'}}{\sqrt[4]{ \mathcal{K} }}$	$\operatorname{arccns} \frac{\sqrt{k}}{\sqrt[4]{ \mathcal{K} }}$
$h(\kappa)$	$\sqrt{k/k'}$	$\sqrt{1/k'}$	$\sqrt{k}$
$u_0$	$\operatorname{arccn} \frac{q_0}{h(\kappa) \sqrt[4]{ \mathcal{K} }}$	$\operatorname{arcdn} \frac{q_0}{h(\kappa) \sqrt[4]{ \mathcal{K} }}$	$\operatorname{arcsn} \frac{q_0}{h(\kappa) \sqrt[4]{ \mathcal{K} }}$

TABLE I. Elliptic parametrization of stable trajectories of McMillan octupole map (after [9]);  $\eta_- = 2\mathcal{K}[\kappa] - \eta_+$ .

Using parametrization of individual curves, we now can compute the action integral [14] as

$$J = \frac{1}{2\pi} \oint p dq = \frac{\sqrt{|\mathcal{K}|}}{2\pi} \times \begin{cases} \kappa S_{\text{sn}}, \\ (\kappa/\kappa') S_{\text{cn}}, \\ (1/\kappa') S_{\text{dn}}, \end{cases}$$

where  $S_{\text{ef}}$  are areas of *elliptic Lissajous curves* with equal frequencies and phase difference  $\eta$  (see Appendix B):

$$J_{\text{sn}} = \frac{2}{\pi} \frac{\sqrt{|\mathcal{K}|}}{\kappa} \frac{1}{\operatorname{sn}^3 \eta} \left\{ -\operatorname{dn}^2 \eta \operatorname{K}[\kappa] + \operatorname{sn}^2 \eta \operatorname{E}[\kappa] + \operatorname{cn}^2 \eta \operatorname{dn}^2 \eta \operatorname{II}[k^2 \operatorname{sn}^2 \eta, \kappa] \right\},$$

$$J_{\text{cn}} = \frac{2}{\pi} \frac{\sqrt{|\mathcal{K}|}}{\kappa \kappa'} \frac{\operatorname{dn} \eta}{\operatorname{sn}^3 \eta} \left\{ \operatorname{K}[\kappa] - \operatorname{sn}^2 \eta \operatorname{E}[\kappa] - \operatorname{cn}^2 \eta \operatorname{II}[k^2 \operatorname{sn}^2 \eta, \kappa] \right\},$$

$$J_{\text{dn}} = \frac{1}{\pi} \frac{\sqrt{|\mathcal{K}|}}{\kappa'} \frac{\operatorname{cn} \eta}{\operatorname{sn}^3 \eta} \left\{ (\operatorname{sn}^2 \eta + \operatorname{dn}^2 \eta) \operatorname{K}[\kappa] - \operatorname{sn}^2 \eta \operatorname{E}[\kappa] - \operatorname{dn}^2 \eta \operatorname{II}[k^2 \operatorname{sn}^2 \eta, \kappa] \right\}.$$

Figure 7 below shows action-angle variables for McMillan octupole map for different values of parameters  $a$  and  $\Gamma$ .

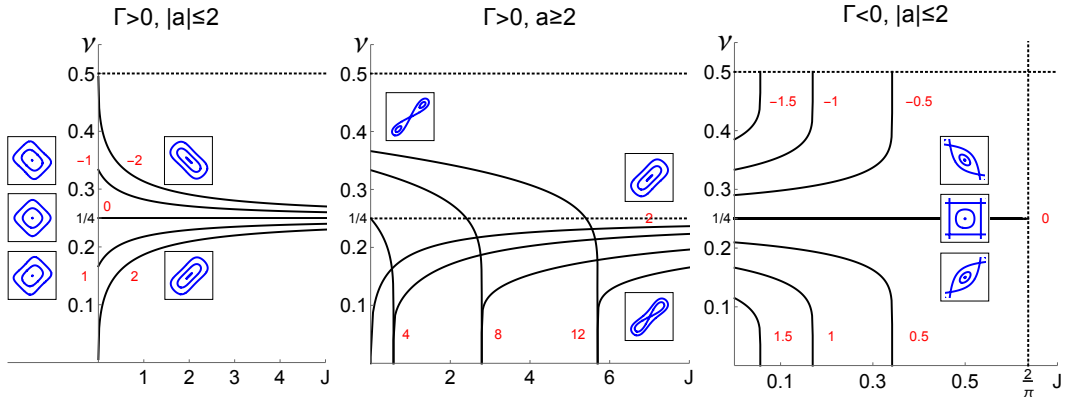


FIG. 7. Action-angle variables for the McMillan octupole map for different values of  $a$  (red labels) and  $|\Gamma| = 1$ . Each plot corresponds to a different regime of oscillations: the left plot shows regime with single fixed point, the one in the middle is regime with lemniscate, and regime with finite dynamical aperture ( $\Gamma < 0$ ) is on the right.

## V. APPLICATIONS OF MCMILLAN MAP

Besides the obvious importance of McMillan map as one of very few known exact integrable models (e.g. see [15] for the short review on integrability of symplectic maps of the plane), it has a much deeper meaning. In order to see that, we first should comment on a McMillan-Turaev form of the map

$$\begin{aligned}\mathcal{M}_{\text{MT}} : q' &= p, \\ p' &= -q + f(p).\end{aligned}$$

At first glance the map might look very restrictive; McMillan's original idea was based on its simplicity and clear symmetries, while still having some degree of freedom in modifying the dynamics by varying only  $f(p)$ . As it was demonstrated later by D. Turaev [16], any symplectic  $2n$ -D mapping can be approximated to the MT form up to a given numerical precision. Thus, in a certain sense, MT form is the canonical form for all symplectic maps with differentiable  $f(p)$ . In next few subsections we show that McMillan sextupole and octupole maps are at the core of general MT map and will propose a natural extension of the optical function formalism used in accelerator physics. While material below requires its own publication, which we will make soon, we briefly describe main ideas.

### A. McMillan map and perturbation theory

Consider the general map in MT form with  $f(p)$  being differentiable function of its argument. Without loss of generality we will assume the fixed point to be at the origin, which requires  $f(0) = 0$ . For an arbitrary otherwise  $f(p)$  the global dynamics is known to be chaotic, except very special integrable cases [7, 8, 15]. As a consequence of KAM theorem [17–19], if linear part of the map is stable

$$|\partial_p f(0)| \leq 2,$$

then there exist an area of quasi-integrable motion around fixed point. Now, we shall introduce a small positive parameter  $\varepsilon$  characterizing the amplitude of oscillations. It can be done using a change of variables  $(q, p) \rightarrow \varepsilon(q, p)$ :

$$\begin{aligned}q' &= p \\ p' &= -q + \frac{1}{\varepsilon} f(\varepsilon p) = -q + a p + \varepsilon \frac{b}{2!} p^2 + \varepsilon^2 \frac{c}{3!} p^3 + \dots\end{aligned}$$

where we expanded the force function in a power series of  $(\varepsilon p)$  and

$$a \equiv \partial_p f(0), \quad b \equiv \partial_p^2 f(0), \quad c \equiv \partial_p^3 f(0), \quad \dots$$

After the introduction of  $\varepsilon$ , one can look for an approximated invariant of motion expanded in powers of a small parameter. In this case, we require the invariant to be conserved to an accuracy of order  $O(\varepsilon^{n+1})$ :

$$\mathcal{K}^{(n)}(p', q') - \mathcal{K}^{(n)}(p, q) = O(\varepsilon^{n+1}). \quad (8)$$

The invariant can be sought in the form of a polynomial

$$\mathcal{K}^{(n)} = \mathcal{K}_0 + \varepsilon \mathcal{K}_1 + \varepsilon^2 \mathcal{K}_2 + \dots + \varepsilon^n \mathcal{K}_n,$$

with  $\mathcal{K}_m$  being homogeneous polynomials in  $p$  and  $q$  of  $(m+2)$  degree:

$$\begin{aligned}\mathcal{K}_0 &= C_{2,0} p^2 + C_{1,1} p q + C_{0,2} q^2, \\ \mathcal{K}_1 &= C_{3,0} p^3 + C_{2,1} p^2 q + C_{1,2} p q^2 + C_{0,3} q^3, \\ &\dots,\end{aligned}$$

and  $C_{i,j}$  are coefficients to be determined in order to satisfy Eq. (8). Leaving it to a reader to verify, we will provide a general result. In first order of such a perturbation theory we have

$$\mathcal{K}(p, q) = p^2 - a p q + q^2 - \frac{b}{2!} \frac{p q (p+q)}{a-1} \varepsilon + O(\varepsilon^2). \quad (9)$$

In the case if  $f(p)$  is an even function of its argument (or just  $b = 0$ ), the expansion begins from the next order and we have

$$\mathcal{K}(p, q) = p^2 - a p q + q^2 - \frac{c}{3!} \frac{p^2 q^2}{a} \varepsilon^2 + C (p^2 - a p q + q^2)^2 \varepsilon^2 + O(\varepsilon^3), \quad (10)$$

where  $C$  is a coefficient such that Eq. (8) is satisfied for any value of  $C$ .

Here one can recognize (if we set  $C = 0$  in Eq. (10)) that these are invariants of McMillan sextupole and octupole maps. Thus we learn that these McMillan mappings, are not just two integrable systems; in the same way the quadratic invariant

$$\mathcal{K}^{(0)}(p, q) = p^2 - a p q + q^2$$

and linear force  $f(p) = a p$  describe the dynamics around the fixed point of a general dynamical systems in the zeroth order (known as linearization), McMillan sextupole and octupole maps with invariants  $\mathcal{K}_{\text{sex,oct}}$  provide the next order approximation. As a result one can “integrate out” additional dynamical properties, such as action-angle dependence and even boundary of stability around some major resonances. After the truncation of force function at the second order one produces new dynamical system which is chaotic again (quadratic or cubic Hénon maps). However addition of higher order terms according to Eqs. (2) and (3) matches the force with invariant producing nonlinear integrable map.

Another famous chaotic dynamical system we would like to use as an example is *Chirikov map* [20, 21] (also known as *Chirikov standard* or *Chirikov-Taylor map*). In accelerator physics it is used to model longitudinal dynamics in a ring with single thin RF station, and in MT form is given by

$$\begin{aligned} q' &= p, \\ p' &= -q + 2p - K \sin p. \end{aligned}$$

This map has an approximated invariant in the octupole form (10) with  $a = 2 - K$  and  $c = K$ .

## B. Nonlinear Twiss parameters

Now let us consider a simple accelerator lattice with 1 degree of freedom consisting of elements of linear optics (drift spaces, dipoles and quadrupoles) and a single thin nonlinear lens:

$$\mathbb{F}: \begin{bmatrix} x \\ \dot{x} \end{bmatrix}' = \begin{bmatrix} x \\ \dot{x} \end{bmatrix} + \begin{bmatrix} 0 \\ F(x) \end{bmatrix}.$$

The action on a test particle from all linear elements can be represented using matrix with Courant-Snyder parametrization [22]

$$\mathbb{M}: \begin{bmatrix} x \\ \dot{x} \end{bmatrix}' = \begin{bmatrix} \cos \Phi + \alpha \sin \Phi & \beta \sin \Phi \\ -\gamma \sin \Phi & \cos \Phi - \alpha \sin \Phi \end{bmatrix} \begin{bmatrix} x \\ \dot{x} \end{bmatrix},$$

where  $\alpha$ ,  $\beta$  and  $\gamma$  are *Twiss parameters* (also known as *Courant-Snyder parameters*) at the thin lens location, and,  $\Phi$  is the *betatron phase advance* over linear optics insert

$$\Phi = \int \frac{ds}{\beta(s)}.$$

Without nonlinear lens Twiss parameters are functions of longitudinal coordinate  $s$  with  $\beta(s)$  refereed as  $\beta$ -function,  $\alpha(s) \equiv -\dot{\beta}(s)/2$  and  $\gamma(s) \equiv [1 + \alpha^2(s)]/\beta(s)$ . At any location the *Courant-Snyder invariant* is defined as

$$\gamma(s) x^2(s) + 2\alpha(s) x(s) \dot{x}(s) + \beta(s) \dot{x}^2(s) = \text{const}$$

and rotation number (or *betatron tune* in accelerator physics) is independent of amplitude and given by

$$\nu = \frac{1}{2\pi} \oint \frac{ds}{\beta(s)}.$$

When the nonlinear lens is introduced, the combined one-turn map  $M \circ F$  can be rewritten in MT form using change of variables

$$\begin{cases} q = x, \\ p = x (\cos \Phi + \alpha \sin \Phi) + \dot{x} \beta \sin \Phi, \end{cases}$$

with force function being

$$f(q) = 2q \cos \Phi + \beta \sin \Phi F(q).$$

Using results from the previous subsection we know that we can define an approximated invariant

$$\mathcal{K}(p, q) \approx \text{C.S.} - \frac{b}{2!} \frac{\Pi \Sigma}{a-1}$$

or if  $b = 0$

$$\mathcal{K}(p, q) \approx \text{C.S.} - \frac{c}{3!} \frac{\Pi^2}{a},$$

where we used our symmetric notations  $\text{C.S.} \equiv p^2 - a p q + q^2$ ,  $\Pi \equiv p q$  and  $\Sigma \equiv p + q$  with

$$a = 2 \cos \Phi + \beta \sin \Phi \partial_q F(0), \quad b = \beta \sin \Phi \partial_{qq} F(0), \quad c = \beta \sin \Phi \partial_{qqq} F(0).$$

New invariant can be easily propagated through the linear part of lattice and defined for any azimuth,  $\mathcal{K}(p, q; s)$ , and if needed  $(q, p)$  can be inverted to physical variables  $(x, \dot{x})$ . Now one can see that coefficients in polynomial invariant can be seen as nonlinear analog of Twiss parameters now including higher order terms. While physical variables are convenient for the representation of final results, all calculations are more convenient in MT form due to the fact that it has clear symmetries, small amount of terms and the only parameters used are intrinsic parameters, such as rotation number at the origin (or  $a$ ) or location of singularities  $\Gamma$ ; MT form and corresponding symmetric invariant is in a way similar to use of Floquet variables, when we remove redundancy in optical functions (since  $\alpha$  and  $\gamma$  are defined through  $\beta$ -function) and use physical variables after we propagate the system in normalized coordinates. We also should briefly note that one can incorporate effect from both, sextupole and octupole, components of nonlinear lens

$$\mathcal{K}(p, q) \approx \text{C.S.} - \frac{b}{2!} \frac{\Pi \Sigma}{a-1} + \left[ \left( \frac{b}{2!} \right)^2 - \frac{c}{3!} \right] \frac{\Pi^2}{a(a-1)},$$

resulting in an additional parameter — the ratio of nonlinear components  $b/c$ . In this case we have a more general symmetric McMillan map invariant level sets of which can be transformed to octupole McMillan map (see [9]).

While conventional Courant-Snyder formalism been successfully used by accelerator community for years, we should remember that it is only linearization ignoring any nonlinear effects and definitely have room for improvement. Suggested nonlinear extension based on McMillan integrable maps has following advantages:

- In traditional Courant-Snyder formalism the rotation number (betatron tune) is independent of amplitude, while in its nonlinear extension we have  $\nu(J) \neq \text{const}$ ; it helps to incorporate chromatic effect of sextupoles and tune shift due to octupoles.
- While linear Courant-Snyder invariant is stable for any amplitude, McMillan invariant introduces dynamical aperture which is quite accurate around resonances of 1-st, 2-nd, 3-rd and 4-th order, respectively  $a = 2, -2, -1$  and  $0$ . In particular the last two resonances plays critical role in sextupole and octupole resonant injection/extraction and new theory provides quick and accurate location of unstable points and separatrices of motion. A specific example is given in next subsection.
- The new formalism is very natural: original invariant is in polynomial form and non-linearities are consistently incorporated. In addition, the new extended invariant again corresponds to exactly integrable system and familiar to accelerator community.

### C. General accelerator lattice

In previous subsection we used a model accelerator with only one nonlinear lens. As a result, we had an ability to analytically convert a one turn map to MT form. But what should we do in the case of general symplectic map of the plane representing more realistic accelerator with multiple nonlinear thin lenses located at different positions along the lattice? Note that thick lenses can always be incorporated into analysis. If for each element of the lattice an exact transformation is known, then one simply expand the full one-turn map into a power series up to the third order, and, if some transformations are unknown one can use symplectic integrator [23] consisting of drifts and thin kicks or Dirac interaction picture along with the Magnus expansion [24].

The first method is to numerically transform the map to MT form using Turaev theorem and thus reduce the analysis to symmetric McMillan mappings. However, one can use the perturbation theory described above for any symplectic map; the only difference is that instead of symmetric one should use general polynomials for the approximated invariant of motion. This approach is less practical in a scenes that asymmetric polynomials have too many coefficients/nonlinear optical functions (4 for sextupole and 5 for octupole). Also note that in general case after the transformation to MT form, the contribution from all sextupoles (and/or sextupole components from other nonlinear lenses) combined in one term of force function; same is true for the octupole component. As reader can guess, in zeroth order one obtain Courant-Snyder invariant, and in first asymmetric McMillan map. This again allows for a quick extraction of aforementioned dynamical properties including structure of the phase space.

In order to illustrate the second approach described above, we will use the example of a third-integer resonant extraction for the Mu2e experiment at Fermilab. Since beam is flat, we will apply our one dimensional theory to the dynamics in horizontal plane  $(x, \dot{x})$ . After producing a one-turn map including all sextupoles and linear optics elements, we expand it in power series and compute zeroth and first order approximated invariants:

$$\mathcal{K}^{(0)}(x, \dot{x}) = 7.29976 \dot{x}^2 - 2.16717 \dot{x}x + 0.250363x^2,$$

$$\mathcal{K}^{(1)}(x, \dot{x}) = \mathcal{K}^{(0)}(x, \dot{x}) - 7.24291 \dot{x}^3 + 5.85441 \dot{x}^2x - 1.00907 \dot{x}x^2 + 0.0338591 x^3.$$

$\mathcal{K}^{(0)}(x, \dot{x})$  is the Courant-Snyder invariant and  $\mathcal{K}^{(1)}(x, \dot{x})$  is in the form of asymmetric McMillan sextupole map. Fig. 8 provides comparison between tracking (using full one-turn map) and approximated invariants. As one can see the dynamic aperture (location of unstable fixed points) and other main features (such as separatrices and shape of stable phase space trajectories) match quite well; without going into details here we will mention that action-angle dependency is also within good accuracy. In an upcoming soon article we will consider in details the application of this theory specifically to accelerator physics considering the range of applicability and several examples demonstrating the validity of estimated dynamical properties.

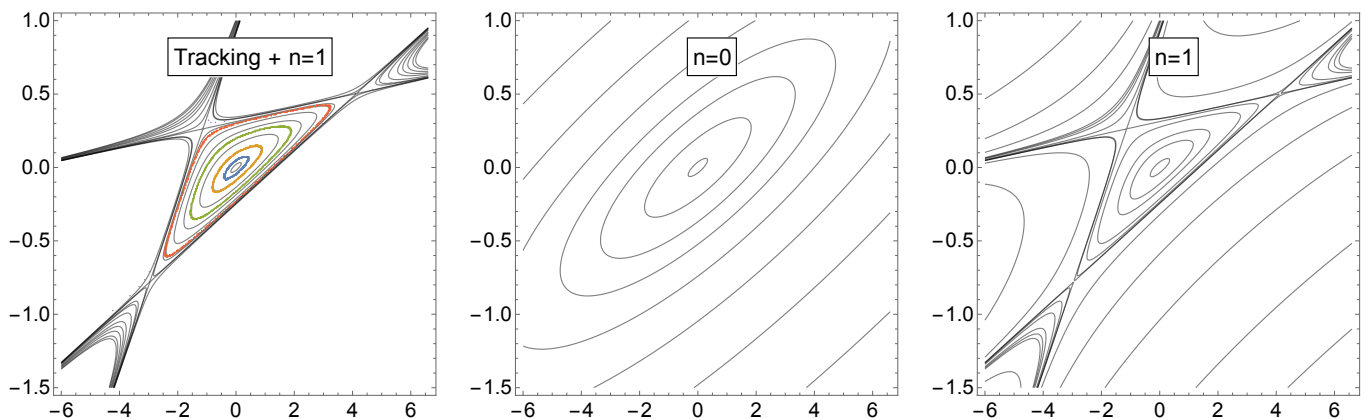


FIG. 8. Left plot provides tracking of the third-integer resonant extraction in horizontal plane for the Mu2e experiment at Fermilab (colored dots); black level sets correspond to nonlinear Courant-Snyder invariant of the first order (shown separately in right plot). Middle and right plots show constant level sets of linear and nonlinear Courant-Snyder invariants,  $\mathcal{K}^{(0)}(x, \dot{x})$  and  $\mathcal{K}^{(1)}(x, \dot{x})$ . All plots are made in physical coordinates  $(x, \dot{x})$ .



## VI. SUMMARY

In this article, we revisited an integrable McMillan map and showed that it is at the core of general symplectic dynamics of the plane. With the help of perturbation theory, we demonstrated that McMillan sextupole and octupole mappings are the first and second order approximations for planar transformations in McMillan-Turaev form. In particular, this allows the natural extension of the optical function formalism used in accelerator physics; this new formalism incorporates the chromatic effect of sextupoles and tune shift due to octupole magnets, along with dynamical aperture around low order resonances. As an example, we used a real accelerator lattice used for the Mu2e experiment at Fermilab, which revealed a great correspondence between tracking and perturbation theory applied for the third-order resonant extraction.

This manuscript is first in a series of publications dedicated to McMillan map and related integrable systems in higher dimensions with its applications to accelerator physics. In this work, we provide a systematic description of basic underlying ideas: in particular, we give a complete description of all stable trajectories, including bifurcation diagrams, parametrization of invariant curves (see [9]), Poincaré rotation numbers, and canonical action-angle variables.

## VII. ACKNOWLEDGMENTS

The authors would like to thank Eric Stern (FNAL) and Taylor Nchako (Northwestern University) for carefully reading this manuscript and for their helpful comments. Moreover, we would like to extend our gratitude to Vladimir Nagaslaev (FNAL) for multiple discussions and his generous contributions in preparation of Fig. 8.

This research is supported by Fermi Research Alliance, LLC under Contract No. DE-AC02-07CH11359 with the U.S. Department of Energy and by the University of Chicago.

**Appendix A: Stability of fixed points and 2-cycles for  
McMillan sextupole and octupole mappings**

In this appendix we provide tables with stability domain for fixed points and two-cycles of the integrable McMillan sextupole and octupole mappings.

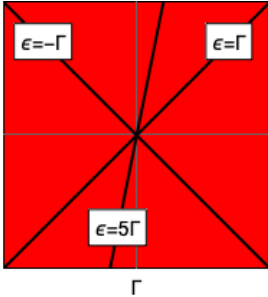
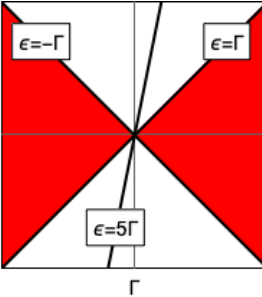
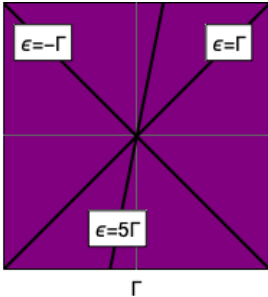
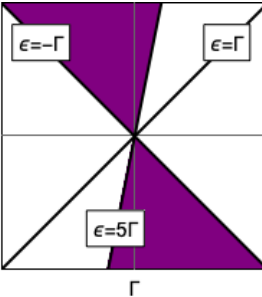
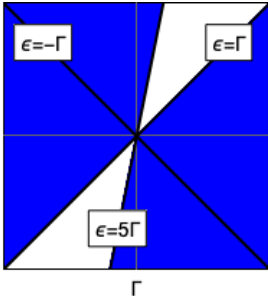
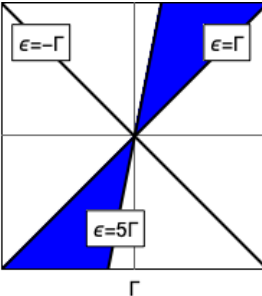
	$\mathcal{K}(\zeta)$	Domain $\zeta \in \mathbb{R}^2$	Stability domain
$\zeta^{(1-1)}$	0	$\mathbb{R}^2$	$(\Gamma + \epsilon)(\Gamma - \epsilon) > 0$
			
$\zeta^{(1-2)}$	$\frac{8}{27}(\Gamma + \epsilon)^3$	$\mathbb{R}^2$	$(\Gamma + \epsilon)(5\Gamma - \epsilon) < 0$
			
$\zeta^{(2)}$	$4\Gamma(\Gamma - \epsilon)^2$	$(\Gamma - \epsilon)(5\Gamma - \epsilon) > 0$	$(\Gamma - \epsilon)(5\Gamma - \epsilon) < 0$
			

TABLE II. Value of the invariant,  $\mathcal{K}_{\text{sex}}(\zeta)$ , domain where point is real and its stability domain for fixed points and two-cycles of the McMillan sextupole map.

	$\mathcal{K}(\zeta)$	Domain $\zeta \in \mathbb{R}^2$	Stability domain
$\zeta^{(1-1)}$	0	$\mathbb{R}^2$	$(\Gamma + \epsilon)(\Gamma - \epsilon) > 0$
$\zeta^{(1-2,3)}$	$-(\Gamma + \epsilon)^2$	$\epsilon < -\Gamma$	$\Gamma(\Gamma + \epsilon) < 0$
$\zeta^{(2)}$	$-(\Gamma - \epsilon)^2$	$\epsilon > \Gamma$	$\Gamma(\Gamma - \epsilon) < 0$

TABLE III. Value of the invariant,  $\mathcal{K}_{\text{oct}}(\zeta)$ , domain where point is real and its stability domain for fixed points and two-cycles of the McMillan octupole map.

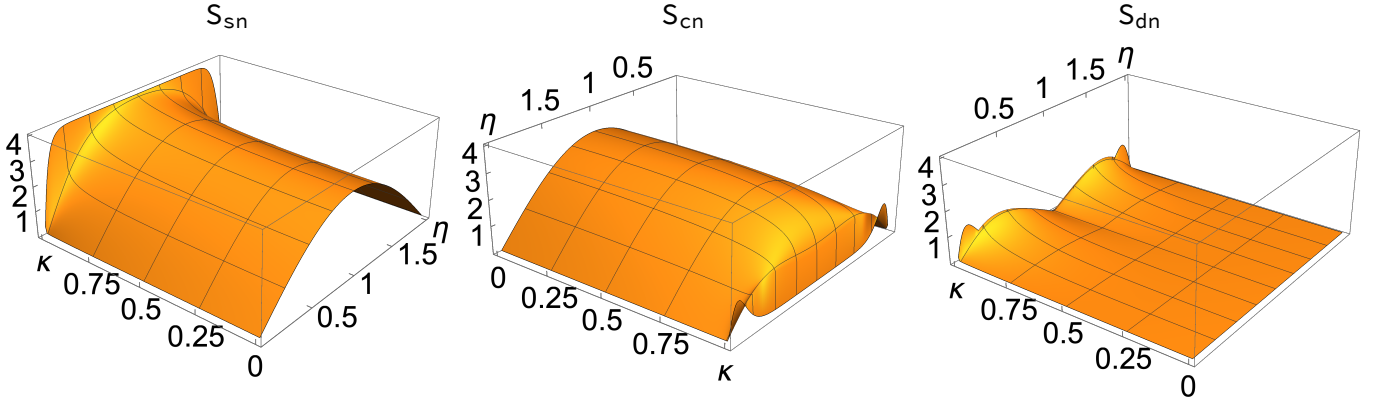


FIG. 9. Area under the closed elliptic Lissajous curve for major elliptic functions and unit ratio ( $\omega_1 : \omega_2 = 1$ ) as a function of modulus  $\kappa$  and phase difference  $\eta$ . Note that  $\eta$  is measured in units of quarter period  $K[\kappa]$ .

### Appendix B: Elliptic Lissajous figures

Traditionally a *Lissajous figure* (or curve) is the graph defined by the parametric set of equations

$$\begin{aligned} x &= \sin(\omega_1 t), \\ y &= \sin(\omega_2 t + \eta). \end{aligned}$$

A natural extension is substitution of Jacobi elliptic functions instead of trigonometric

$$\begin{aligned} x &= \text{ef}(\omega_1 t, \kappa), \\ y &= \text{ef}(\omega_2 t + \eta, \kappa). \end{aligned}$$

We will define graph of this parametric set as *Lissajous-Jacobi curve* or *elliptic Lissajous figure*; one can think of even further generalization by using two different elliptic functions, e.g. sn vs. cn, which we will not consider.

In this article we are mainly interested in closed curves with unit ratio,  $\omega_1 : \omega_2 = 1$ , and especially the area they enclose. Area can be found using the integral  $S = \oint y dx$  resulting in

$$\begin{aligned} S_{\text{sn}} &= \frac{4}{\kappa^2} \frac{1}{\text{sn}^3 \eta} \left\{ -\text{dn}^2 \eta K[\kappa] + \text{sn}^2 \eta E[\kappa] + \text{cn}^2 \eta \text{dn}^2 \eta \Pi[k^2 \text{sn}^2 \eta, \kappa] \right\}, \\ S_{\text{cn}} &= \frac{4}{\kappa^2} \frac{\text{dn} \eta}{\text{sn}^3 \eta} \left\{ K[\kappa] - \text{sn}^2 \eta E[\kappa] - \text{cn}^2 \eta \Pi[k^2 \text{sn}^2 \eta, \kappa] \right\}, \\ S_{\text{dn}} &= 2 \frac{\text{cn} \eta}{\text{sn}^3 \eta} \left\{ (\text{sn}^2 \eta + \text{dn}^2 \eta) K[\kappa] - \text{sn}^2 \eta E[\kappa] - \text{dn}^2 \eta \Pi[k^2 \text{sn}^2 \eta, \kappa] \right\}. \end{aligned}$$

Figure 9 illustrates behavior of area as a function of  $\eta$  and  $\kappa$ . Figures 10 – 12 show examples of Lissajous-Jacobi figures for major elliptic functions sn, cn and dn. For all plots  $\eta$  is measured in  $K[\kappa]$  known as the quarter period and being the complete elliptic integral of the first kind.

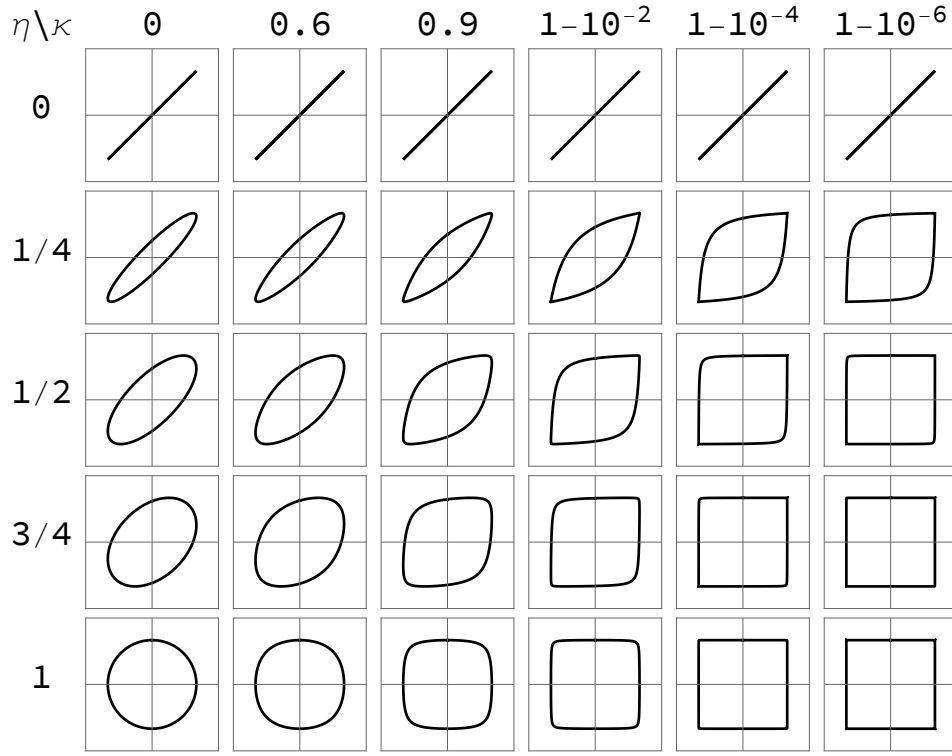


FIG. 10. Lissajous-Jacobi figures (sn vs. sn) for a unit ratio,  $\omega_1 : \omega_2 = 1$ . Columns and rows corresponds to different values of elliptic modulus  $\kappa$  and phase difference  $\eta$ . Note that  $\eta$  is measured in units of quarter period  $K[\kappa]$ .

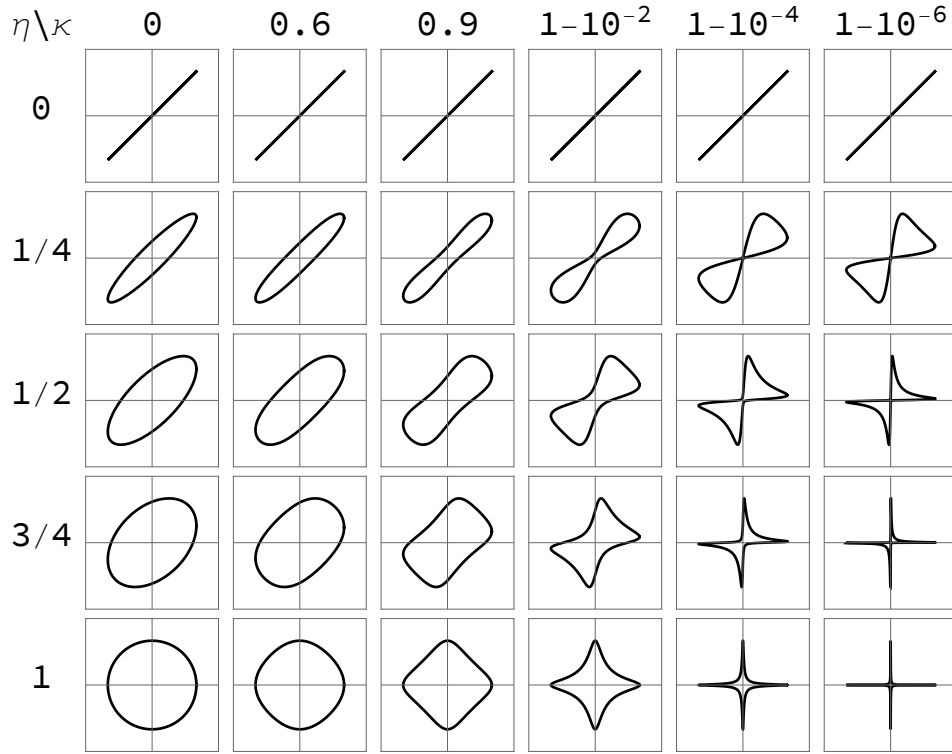


FIG. 11. Lissajous-Jacobi figures (cn vs. cn) for a unit ratio,  $\omega_1 : \omega_2 = 1$ . Columns and rows corresponds to different values of elliptic modulus  $\kappa$  and phase difference  $\eta$ . Note that  $\eta$  is measured in units of quarter period  $K[\kappa]$ .

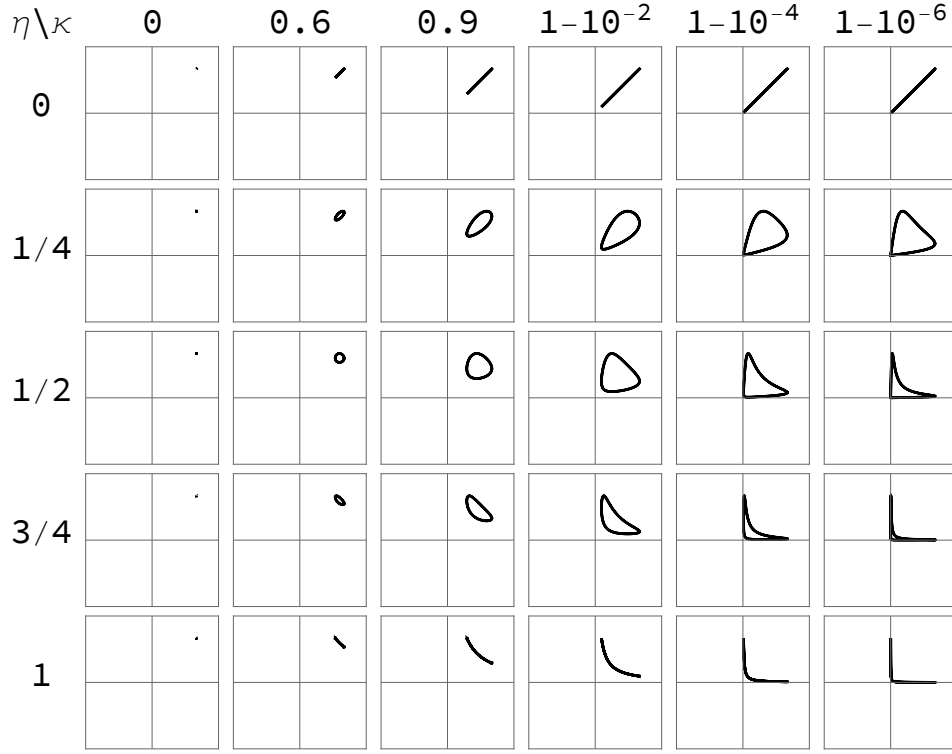


FIG. 12. Lissajous-Jacobi figures (dn vs. dn) for a unit ratio,  $\omega_1 : \omega_2 = 1$ . Columns and rows corresponds to different values of elliptic modulus  $\kappa$  and phase difference  $\eta$ . Note that  $\eta$  is measured in units of quarter period  $K[\kappa]$ .

- 
- [1] V. Alexeev, Bull. Inst. Theoret. Astron **10**, 241 (1965).  
[2] C. Marchal, Bulletin Astronomique **1**, 189 (1966).  
[3] C. Marchal, Celestial mechanics **38**, 377 (1986).  
[4] M. M. Jakas, Physical Review A **52**, 866 (1995).  
[5] M. M. Jakas, Nuclear Instruments and Methods in Physics Research Section B: Beam Interactions with Materials and Atoms **115**, 255 (1996).  
[6] M. P. Strand and W. P. Reinhardt, The Journal of Chemical Physics **70**, 3812 (1979).  
[7] E. M. McMillan, in *Topics in modern physics, a tribute to E. V. Condon*, edited by E. Brittin and H. Odabasi (Colorado Associated University Press, Boulder, CO, 1971) pp. 219–244.  
[8] Y. B. Suris, Functional Analysis and Its Applications **23**, 74 (1989).  
[9] A. Iatrou and J. A. G. Roberts, **15**, 459 (2002).  
[10] B. Cathey, G. Stancari, A. Valishev, and T. Zolkin, Journal of Instrumentation **16**, P03041 (2021).  
[11] M. Henon, Quarterly of applied mathematics, 291 (1969).  
[12] T. Zolkin, S. Nagaitsev, and V. Danilov, arXiv preprint arXiv:1704.03077 (2017).  
[13] S. Nagaitsev and T. Zolkin, Physical Review Accelerators and Beams **23**, 054001 (2020).  
[14] T. Zolkin and S. Nagaitsev, (2016).  
[15] T. Zolkin, Y. Kharkov, and S. Nagaitsev, arXiv preprint arXiv:2201.13133 (2022).  
[16] D. Turaev, Nonlinearity **16**, 123 (2002).  
[17] A. N. Kolmogorov, in *Dokl. Akad. Nauk SSSR (NS)*, Vol. 98 (1954) pp. 527–530.  
[18] J. K. Moser, Matematika **6**, 51 (1962).  
[19] V. Arnol'd, Uspekhi Mat. Nauk **18**, 13 (1963).  
[20] B. Chirikov, Nuclear Physics, Novosibirsk.(Engl. Trans. CERN Transl. 31, 1971) (1969).  
[21] B. V. Chirikov, Physics reports **52**, 263 (1979).  
[22] E. D. Courant and H. S. Snyder, Annals of physics **3**, 1 (1958).  
[23] H. Yoshida, Physics letters A **150**, 262 (1990).  
[24] I. Morozov and E. Levichev, CERN Proceedings **1**, 195 (2017).